

Two-Phase Wall Friction Model for the TRACE Computer Code

Joseph M. Kelly

*U.S. Nuclear Regulatory Commission
11545 Rockville Pike, MS T-10K8
Rockville, Maryland 20852-2738
Phone: (301)415-6852 Fax: (301)415-5160
email: jmk1@nrc.gov*

Weidong Wang

*U.S. Nuclear Regulatory Commission
11545 Rockville Pike, MS T-10K8
Rockville, Maryland 20852-2738
Phone: (301)415-6852 Fax: (301)415-5160
email: wxw1@nrc.gov*

Keywords: Thermal-hydraulics, reactor, model, code

Abstract

The wall drag model in the TRAC/RELAP5 Advanced Computational Engine computer code (TRACE) has certain known deficiencies. For example, in an annular flow regime, the code predicts an unphysical high liquid velocity compared to the experimental data. To address those deficiencies, a new wall frictional drag package has been developed and implemented in the TRACE code to model the wall drag for two-phase flow system code. The modeled flow regimes are (1) annular/mist, (2) bubbly/slug, and (3) bubbly/slug with wall nucleation. The new models use void fraction (instead of flow quality) as the correlating variable to minimize the calculation oscillation. In addition, the models allow for transitions between the three regimes. The annular/mist regime is subdivided into three separate regimes for pure annular flow, annular flow with entrainment, and film breakdown. For adiabatic two-phase bubbly/slug flows, the vapor phase primarily exists outside of the boundary layer, and the wall shear uses single-phase liquid velocity for friction calculation. The vapor phase wall friction drag is set to zero for bubbly/slug flows. For bubbly/slug flows with wall nucleation, the bubbles are presented within the hydrodynamic boundary layer, and the two-phase wall friction drag is significantly higher with a pronounced mass flux effect. An empirical correlation has been studied and applied to account for nucleate boiling. Verification and validation tests have been performed, and the test results showed a significant code improvement.

1. Introduction

The TRAC/RELAP5 Advanced Computational Engine computer code (TRACE) [Ref. 1] is a consolidated thermal-hydraulics reactor system code, developed by the U.S. Nuclear Regulatory Commission (NRC). As such, the TRACE code provides advanced best-estimate simulations of real and postulated transients in pressurized- and boiling-water reactors (PWRs and BWRs, respectively) for many thermal-hydraulics facilities. As a result, the NRC uses the TRACE code for reactor safety audit calculations, and the nuclear power industry and research institutes use the code for reactor system safety studies.

The fundamental theory underlying the TRACE code is based on the two-phase two-fluid model and its constitutive relations. Given that foundation, certain deficiencies have been observed in its two-phase wall friction model. For example, in an annular flow regime, the code predicts unphysical high liquid velocity compared to the experimental data. The annular flow regime is important in many reactor safety simulations, such as modeling condensation on vertical surfaces — a phenomenon important to the operation of passive cooling systems in advanced light-water reactors, such as the containment cooling system in the General Electric Economic and Simplified Boiling-Water Reactor (ESBWR). Further investigation revealed that this deficiency is attributable to improper wall drag modeling.

In the original TRACE model, the wall friction drag is partitioned between vapor and liquid phases and, at high void fraction, the wall drag is primarily distributed to the vapor phase. Consequently, prediction of liquid velocity in a downward annular flow resulted in a predicted film thickness that was more than an order of magnitude smaller than experimental data. As a result, the original code cannot correctly predict the heat transfer phenomenon in the annular flow regime. Moreover, the partitioning of the wall drag in the original code does not represent the correct physics, given that the flow is separated in annular flow, and only the liquid is in contact with the wall in bubbly and annular flow regimes. In other flow regimes, the original wall friction model used flow quality as the correlating variable, and this may cause flow oscillation in calculations. This paper reviews the original model in the TRACE code and proposes a new set of wall drag models to address the deficiencies.

2. Original TRACE Formulation

The TRACE code is based on a two-phase two-fluid model, with the following field equations for liquid and combined gases:

$$\begin{aligned} \frac{\partial \vec{V}_l}{\partial t} + \vec{V}_l \cdot \nabla \vec{V}_l = & -\frac{1}{\rho_l} \nabla P - \frac{C_i}{(1-\alpha)\rho_l} (\vec{V}_g - \vec{V}_l) |\vec{V}_g - \vec{V}_l| \\ & - \frac{\Gamma^+}{(1-\alpha)\rho_l} (\vec{V}_g - \vec{V}_l) - \frac{C_{wl}}{(1-\alpha)\rho_l} \vec{V}_l |\vec{V}_l| + \vec{g} \end{aligned} \quad (2.1)$$

and

$$\begin{aligned} \frac{\partial \vec{V}_g}{\partial t} + \vec{V}_g \cdot \nabla \vec{V}_g = & -\frac{1}{\rho_g} \nabla P - \frac{C_i}{\alpha\rho_g} (\vec{V}_g - \vec{V}_l) |\vec{V}_g - \vec{V}_l| \\ & - \frac{\Gamma^+}{\alpha\rho_g} (\vec{V}_g - \vec{V}_l) - \frac{C_{wg}}{\alpha\rho_g} \vec{V}_g |\vec{V}_g| + \vec{g} \end{aligned} \quad (2.2)$$

where C_i is the interfacial friction factor and C_{wf} and C_{wg} are wall drag coefficients, which are defined as follows:

$$\begin{aligned} C_{wl} &= \frac{(1-\alpha) \cdot \rho_l \cdot C_{fl}}{D_h} \\ C_{wg} &= \frac{\alpha \cdot \rho_g \cdot C_{fg}}{D_h} \end{aligned} \quad (2.3)$$

C_{fl} and C_{fg} in equation (2.3) relate to the two-phase friction factor and are defined as follows:

$$\begin{aligned} C_{fl} &= \frac{2 \cdot f_{2\phi l}}{(1-\alpha)} \\ C_{fg} &= \frac{2 \cdot f_{2\phi g}}{\alpha} \end{aligned} \quad (2.4)$$

The original TRACE code calculated the friction factor using the Churchill correlation [Ref. 2]. However, it also used a two-phase homogeneous wall drag model to compute the wall friction factor, and set the liquid and gas wall frictions to equal values. This modeling practice does not represent the correct physics, given that only the liquid is in contact with the wall in bubbly and annular flow regimes.

In the model development that follows, a two-phase friction factor, $f_{2\phi}$, is defined for each phase. These two-phase friction factors already contain an effective two-phase multiplier and relate to the TRACE variables by equation (2.4).

3. Flow Regimes To Be Modeled

The flow regimes to be modeled are (1) annular/mist, (2) bubbly/slug, (3) bubbly/slug with wall nucleation, and (4) bubbly/slug with ‘‘hot wall.’’ In addition, the model must allow for transitions between these regimes using the following simple criteria:

$\alpha \geq 0.9$:	annular/mist
$\alpha \leq 0.8$:	bubbly/slug
$0.8 < \alpha < 0.9$:	transition from bubbly/slug to annular/mist

4. Annular/Mist Flow Regime

This section begins by describing the two-phase wall drag model for pure annular flow. It then examines the complications arising from the presence of entrained drops or a partially wetted condition.

Pure Annular Flow

Annular flow is the most amenable to analytical modeling and, hence, provides a good starting point. The available literature offers a profusion of two-phase multipliers to account for the enhancement of wall drag.

The multiplier used here applies to the “liquid phase flowing alone,” as follows:

$$\Phi_l^2 = \left(\frac{dP}{dz} \Big|_f \right) / \left(\frac{dP}{dz} \Big|_f \right)_l \quad (4.1)$$

where

$$\left(\frac{dP}{dz} \Big|_f \right)_l = \frac{4 \cdot f_l \cdot 1}{D_h} \cdot \frac{G_l^2}{2 \cdot \rho_l} \quad (4.2)$$

G_l is the mass flux of the liquid, and f_l is the single-phase friction factor for the liquid phase flowing alone. That is, use a standard formula for the friction factor as a function of the Reynolds number, and define the liquid Reynolds number as follows:

$$\text{Re}_l = \frac{G_l \cdot D_h}{\mu_l} \quad (4.3)$$

Annular flow theory then gives the two-phase multiplier as follows:

$$\Phi_l^2 = \frac{1}{(1 - \alpha)^2} \quad (4.4)$$

For the new TRACE model, the friction factor for the annular flow regime proposes to use a power law combination of the laminar and turbulent values:

$$f_{film} = (f_{lam}^3 + f_{urb}^3) \quad (4.5)$$

where the laminar value is that for pipe flow

$$f_{lam} = \frac{16}{\text{Re}_l} \quad (4.6)$$

and the turbulent (by Haaland’s explicit approximation to the Colebrook equation) is as follows:

$$f_{urb} = 1 / \left\{ 3.6 \cdot \log_{10} \left[\frac{6.9}{\text{Re}_l} + \left(\frac{\varepsilon/D}{3.7} \right)^{1.11} \right] \right\}^2 \quad (4.7)$$

Note that the roughness effect has not been conclusively established for annular flow. It is included here to provide a continuous description with that for single-phase flow.

With the friction factor defined by equation (4.5), the two-phase friction factors for annular flow are as follows:

$$\begin{aligned} f_{2\Phi,l} &= f_{film} \\ f_{2\Phi,g} &= 0 \end{aligned} \quad (4.8)$$

Annular Flow with Entrainment

Annular flow with entrainment is treated in a similar manner, with the exception that the wall drag is only computed for the liquid flowing in the film (not for the total liquid flow rate). Thus, equation (4.2) is modified, as follows:

$$\left(\frac{dP}{dz} \Big|_f \right)_l = \frac{4 \cdot f_l \cdot 1}{D_h} \cdot \frac{G_{film}^2}{2 \cdot \rho_l} = \frac{4 \cdot f_l \cdot 1}{D_h} \cdot \frac{(1 - \varepsilon)^2 \cdot G_l^2}{2 \cdot \rho_l} \quad (4.9)$$

where ε is the fraction of the entrained liquid. The friction factor for the annular film is then calculated as before, with the liquid film Reynolds number given by the following equation:

$$\text{Re}_l = \frac{G_{film} \cdot D_h}{\mu_l} = \frac{(1 - \varepsilon) \cdot G_l \cdot D_h}{\mu_l} \quad (4.10)$$

After determining the film friction factor using equations (4.5) and (4.10), the two-phase friction factors are as follows:

$$\begin{aligned} f_{2\Phi,l} &= (1 - \varepsilon)^2 \cdot f_{film} \\ f_{2\Phi,g} &= 0 \end{aligned} \quad (4.11)$$

Film Breakdown Regime

An examination of equation (4.11) reveals that the wall drag to the liquid phase (film) disappears as the entrained fraction goes to unity, as expected. However, wall drag to the gas phase should commence (at some point) as the liquid film disappears. The concept of a minimum film thickness accomplishes this transition in a natural way. That is, when film breakdown occurs, the resulting rivulets are assumed to have a thickness equal to the minimum value. Then, using the thin film approximation, the wetted fraction of the surface is given by the following equation:

$$f_{wet} = \frac{(1 - \alpha)_{film} \cdot D_h}{4 \cdot \delta_{min}} \quad (4.12)$$

Equation (4.12) uses the volume fraction of the liquid film. However, the liquid film volume fraction is not calculated and can only be approximated until the droplet field is incorporated into TRACE,. Thus, the following equation provides a suitable approximation for the purpose of providing a ramp to turn on wall drag to the gas phase:

$$(1-\alpha)_{film} = (1-\varepsilon) \cdot (1-\alpha) \quad (4.13)$$

yielding

$$f_{wet} = (1-\varepsilon) \cdot \frac{(1-\alpha) \cdot D_h}{4 \cdot \delta_{min}} \quad (4.14)$$

The film breakdown regime is considered to exist whenever the liquid film thickness falls below the specified minimum value. Again, using the thin film approximation, the film thickness is as follows:

$$\delta = (1-\varepsilon) \cdot \frac{(1-\alpha) \cdot D_h}{4} \quad (4.15)$$

The wetted fraction can then be rewritten as follows:

$$f_{wet} = \frac{\delta}{\delta_{min}} \quad (4.16)$$

For the present, a simple constant value of 50 microns is used.

After determining that the film breakdown regime has been entered and calculating the wetted fraction of the surface, we must specify the two-phase friction factors. Thus, the drag between the wall and the liquid phase is computed as before and applied to the wetted fraction, as follows:

$$f_{2\phi,l} = f_{wet} \cdot (1-\varepsilon)^2 \cdot f_{film} \quad (4.17)$$

Similarly, the drag between the wall and the gas phase is computed and applied to the wetted fraction, as follows:

$$f_{2\phi,g} = (1-f_{wet}) \cdot f_{1\phi,g} \quad (4.18)$$

and the single-phase gas friction factor is calculated using the Churchill correlation [Ref. 2] with the gas Reynolds number defined as follows:

$$Re_g = \frac{G_g \cdot D_h}{\mu_g} \quad (4.19)$$

5. Bubbly/Slug Flow Regime

The model for the bubbly slug flow regime is similar to that for the annular/mist regime (as described in Section 4). Ignoring the possibility of entrainment, the frictional pressure gradient is again given by the following equation:

$$\left(\frac{dP}{dz} \right)_f = \Phi_l^2 \cdot \frac{4 \cdot f_l}{D_h} \cdot \frac{1}{2} \cdot \frac{G_l^2}{\rho_l} \quad (5.1)$$

where two-phase multiplier once again applies to the “liquid flowing alone.” This formulation is then applied, with the friction factor computed using a liquid Reynolds number given by the following equation:

$$Re_l = \frac{G_l \cdot D_h}{\mu_l} \quad (5.2)$$

We then find that the two-phase multiplier for adiabatic (i.e., non-boiling) flows is somewhat lower than that for the annular flow regime. Specifically, using the data of Ferrell and McGee [Ref. 3], we obtain the following “liquid alone” two-phase multiplier for adiabatic flows, as shown in Figure 1:

$$\Phi_l^2 \approx \frac{1}{(1-\alpha)^{1.72}} \quad (5.3)$$

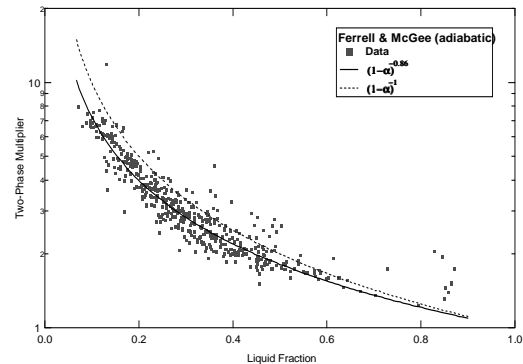


Figure 1: “Liquid alone” two-phase multiplier for the adiabatic data of Ferrell and McGee [Ref. 3].

The behavior of the two-phase multiplier with respect to the liquid fraction depicted in Figure 1 and given by equation (4.2) is very similar to values reported by Yamazaki and Shiba [Ref. 4] and Yamazaki and Yamaguchi [Ref. 5]. Those researchers suggested

exponents of -0.875 for upflow and -0.9 for downflow. Notably, when the data are represented in this way, mass flux, pressure, and tube diameter do not have any noticeable effect.

We can formulate a physical basis for this result, as follows. If the adiabatic two-phase bubbly/slug flow is turbulent, the vapor phase primarily exists outside of the boundary layer. In such instances, the wall shear should be similar to that for a single-phase liquid flow that has the same velocity as the liquid in the two-phase case. Thus, the frictional pressure gradient is as follows:

$$\left(\frac{dP}{dz} \right)_f = \frac{4 \cdot f_{1\Phi,l}}{D_h} \cdot \frac{1}{2} \cdot \rho_l \cdot v_l^2 \quad (5.3)$$

The friction factor is then computed by the single-phase pipe friction correlation, with the Reynolds number defined as follows [instead of using equation (4.3)]:

$$\text{Re}_{1\Phi,l} = \frac{\rho_l \cdot v_l \cdot D_h}{\mu_l} \quad (5.4)$$

The resulting two-phase multiplier for “liquid flowing alone” is as follows:

$$\Phi_l^2 = \frac{f_{1\Phi,l}}{f_l} \cdot \frac{\rho_l \cdot v_l^2}{(G_l^2/\rho_l)} = \frac{f_{1\Phi,l}}{f_l} \cdot \frac{1}{(1-\alpha)^2} \quad (5.5)$$

Now, assume that the relationship between the turbulent friction factor and the Reynolds no. can be represented by the Blasius approximation:

$$f = \frac{0.0791}{\text{Re}^{0.25}} \quad (5.6)$$

Then, substitute equation (5.6) into equation (5.5) for both f_l and $f_{1\Phi,l}$ to yield the following relationship:

$$\Phi_l^2 = \frac{1}{(1-\alpha)^2} \cdot \frac{\text{Re}_l^{0.25}}{\text{Re}_{1\Phi,l}^{0.25}} = \frac{1}{(1-\alpha)^{1.75}} \quad (5.7)$$

Equation (5.7) then provides the physical basis for the bubbly/slug model, and the two-phase friction factors for the bubbly/slug (non-boiling) regime are as follows:

$$\begin{aligned} f_{2\Phi,l} &= f_{1\Phi,l} \\ f_{2\Phi,g} &= 0 \end{aligned}$$

where the liquid single-phase friction factor is calculated using the Churchill correlation [Ref. 2] for

pipe flow, with the Reynolds number defined by equation (5.4).

6. Bubbly/Slug with Wall Nucleation

The situation for a boiling two-phase flow is not entirely clear, as evidenced by Figure 2, which plots the “liquid alone” two-phase multiplier deduced from the boiling data of Ferrell and Bylund [Ref. 6]. Here, the bubbles are present within the hydrodynamic boundary layer. Moreover, for experimental conditions similar to the adiabatic tests of Ferrell and McGee [Ref. 3] discussed above, the two-phase multiplier is significantly higher and contains a pronounced mass flux effect when boiling is present.

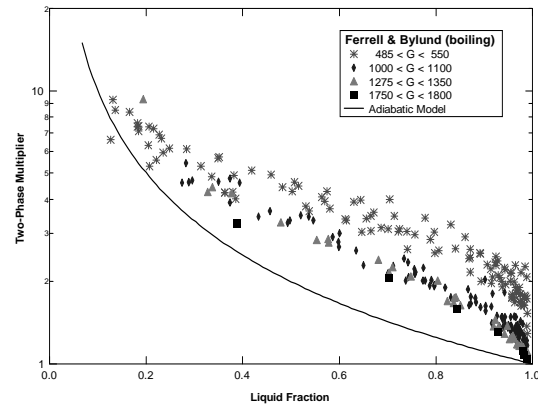


Figure 2: “Liquid alone” two-phase multiplier for boiling data of Ferrell and Bylund [Ref. 6].

No available model for the two-phase multiplier specifically addresses the enhancement attributable to wall nucleation, as illustrated in Figure 2. Collier [Ref. 7] does discuss a surface roughness effect for subcooled boiling, and even suggests that it might be correlated with the bubble departure diameter. However, Collier does not extend this concept into the saturated boiling regime. By contrast, Figure 2 represents both subcooled ($\alpha \leq 0.3$) and saturated ($0.3 < \alpha < 0.8$) boiling data. Note that Figure 2 does not show any evident discontinuity in the behavior of the two-phase multiplier (compared to the liquid fraction) as the saturation line is crossed for a given mass flux.

Consequently, a simple correction factor for the two-phase multiplier for adiabatic two-phase flow is developed using the data of Ferrell and Bylund [Ref. 6]. As suggested by Collier [Ref. 7], we postulated that the correction factor would be a function of the bubble departure diameter. Collier also suggests using the model developed by Levy [Ref. 8], which balances surface tension and drag forces to yield the following relationship:

$$\frac{d_B}{D_h} = 0.015 \cdot \left[\frac{\sigma}{\tau_w \cdot D_h} \right]^{\frac{1}{2}} \quad (6.1)$$

where the wall shear stress is computed without the enhancement attributable to wall nucleation:

$$\tau_w = \frac{f_{\Phi,l}}{2} \cdot \rho_l \cdot v_l^2$$

The bubble diameter then becomes a function of mass flux in addition to pressure.

From an examination of Ferrell and Bylund's data [Ref. 6], we determined that (in addition to the bubble diameter) the proposed correction factor for the enhancement attributable to wall nucleation,

$$\Phi'_l = \Phi_l \cdot (1 + C_{NB}) \quad (6.2)$$

would also have to be a function of void fraction, as depicted in Figure 3. This determination led to the expectation that the wall drag would rapidly be enhanced as bubbles are generated in the subcooled boiling region ($\alpha \approx 0.005$) and then saturate, remaining relatively constant until being suppressed as the liquid layer becomes thinner during the transition to annular flow. Nonetheless, this expectation was defied by the relatively slow increase of the correction factor with void fraction, and peak values at ($\alpha \approx 0.3$); this finding has yet to be explained. Therefore, the resulting model employs a curve fit to model the void fraction dependence, and should be considered empirical in nature. This model is then expressed as follows:

$$C_{NB} = 155 \cdot \left(\frac{d_B}{D_h} \right) \cdot [\alpha \cdot (1 - \alpha)]^{0.62} \quad (6.3)$$

Figure 4 compares the two-phase multipliers computed using this empirical model — equations (6.2) and (6.3) — against the data of Ferrell and Bylund [Ref. 6].

The average error is essentially zero, while the standard deviation is less than 11%.

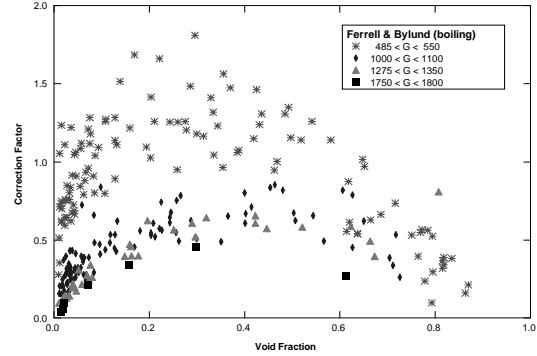


Figure 3: Correction factor for enhancement of the two-phase multiplier attributable to the effects of wall nucleation.

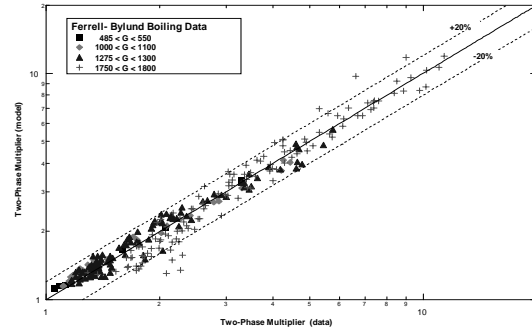


Figure 4: Comparison of calculated and measured two-phase multiplier with the empirical correction factor for the wall nucleation effect.

As with any empirical model, it is necessary to ensure that the model behaves reasonably when extrapolating outside of its database (during a transient system calculation, for example). With respect to pressure, the TRACE database extends from about 4 to 17 bar, so most of the extrapolation is to higher pressures. As the pressure increases, the surface tension decreases (as does the bubble diameter). That decrease, in turn, drives the correction factor to zero as the critical point is approached. This behavior is reasonable and, hence, no explicit limit is needed.

The bubble diameter is also a strong function of liquid mass flux, and the TRACE database extends only from about 500 to 1,800 $\text{kg/m}^2\text{-s}$. As the mass flux increases significantly above the upper limit of

1,800 kg/m²-s, the bubble diameter decreases and the wall nucleation effect disappears, so the two-phase multiplier approaches that for adiabatic flow. Again, this is reasonable behavior and, hence, no explicit limit is needed. However, as the mass flux decreases below the lower limit of 500 kg/m²-s, the bubble diameter rapidly increases. Because the correction factor is directly proportional to bubble diameter, this introduces the possibility that the model may calculate unreasonably large two-phase multipliers. To ensure that this does not occur, it is possible to impose limits on either mass flux or bubble diameter. The simplest approach (and the one recommended here) is to directly limit the correction factor itself, as follows

$$C_{NB} = \text{Min} \left\{ 2, 155 \cdot \left(\frac{d_B}{D_h} \right) \cdot [\alpha \cdot (1 - \alpha)]^{0.62} \right\} \quad (6.4)$$

Finally, the two-phase friction factors for the bubbly/slug regime with wall nucleation are as follows:

$$\begin{aligned} f_{2\Phi,l} &= f_{1\Phi,l} \cdot (1 + C_{NB}) \\ f_{2\Phi,g} &= 0 \end{aligned} \quad (6.5)$$

7. Induced Interfacial Shear

In the code model community, it has been argued that the two-fluid momentum equations should contain a term to account for the “interfacial shear induced by wall shear.” Basically, the idea is that a velocity gradient within the continuous phase attributable to wall shear increases the interfacial force above that for a particle in a uniform velocity field. Despite the lack of direct experimental data, we can formulate a reasonable approximation for this induced shear term by considering the expected behavior in “thought problems,” as follows.

Begin with the one-dimensional, steady-state, two-fluid momentum equations without mass transfer in conservative form:

$$\frac{d}{dz}(\alpha_g \cdot \rho_g \cdot v_g^2) = -\alpha_g \cdot \rho_g \cdot g - \alpha_g \cdot \frac{dP}{dz} - F_{i,drag}''' - F_{wg}''' - F_{i,shear}''' \quad (7.1)$$

and

$$\frac{d}{dz}(\alpha_l \cdot \rho_l \cdot v_l^2) = -\alpha_l \cdot \rho_l \cdot g - \alpha_l \cdot \frac{dP}{dz} + F_{i,drag}''' - F_{wl}''' + F_{i,shear}''' \quad (7.2)$$

where the variables are obvious, with the following exceptions:

$F_{i,drag}'''$: interfacial drag force per unit volume

$F_{i,shear}'''$: interfacial force per unit volume induced by wall shear

F_{wg}''' : wall-gas shear force per unit volume

F_{wl}''' : wall-liquid shear force per unit volume

For these wetted-wall conditions, the wall-gas drag will be zero.

Two-fluid codes do not usually model the interfacial force induced by wall shear. However, for dispersed flows, it is necessary to ensure that thought problems exhibit the expected behavior. To illustrate this point (and find a way to evaluate this term), let’s consider two thought problems:

- (1) In a fully developed, horizontal, bubbly dispersed flow, we expect the continuous liquid and vapor bubbles to have the same velocity, so that the relative velocity and (hence) $F_{i,drag}'''$ will be zero:

$$0 = -\alpha_g \cdot \frac{dP}{dz} - F_{i,shear}'''$$

and

$$0 = -\alpha_l \cdot \frac{dP}{dz} - F_{wl}''' + F_{i,shear}'''$$

Adding these equations together yields the following (expected) relationship:

$$\frac{dP}{dz} = F_{wl}'''$$

Now, multiply the gas equation by the liquid fraction, then multiply the liquid equation by the vapor fraction, and subtract. This yields the following relationship:

$$F_{i,shear}''' = \alpha_g \cdot F_{wl}''' \quad (7.3)$$

Note that without the induced shear term, the relative velocity could not go to zero.

- (2) For a fully developed, vertical, bubbly dispersed flow, we again add the phasic momentum equations to yield the following (expected) relationship:

$$0 = -(\alpha_l \cdot \rho_l + \alpha_g \cdot \rho_g) \cdot g - \frac{dP}{dz} - F_{wl}'''$$

or, more simply,

$$\frac{dP}{dz} = -\rho_m \cdot g - F_{wl}'''$$

If we then repeat the multiplications and subtraction to eliminate the pressure gradient, we obtain the following relationship:

$$0 = \alpha_g \cdot \alpha_l \cdot (\rho_l - \rho_g) \cdot g - F_{i,drag}''' + \alpha_g \cdot F_{wl}''' - F_{i,shear}'''$$

Next, we substitute for the induced shear from equation (7.3), which yields the following:

$$F_{i,drag}''' = \alpha_g \cdot \alpha_l \cdot \Delta\rho \cdot g \quad (7.4)$$

This equation simply states that the interfacial drag force per unit volume is equal to the buoyancy.

Thus, the results from our two thought problems reinforce the concept of the induced shear term and agree that it should be represented as follows:

$$F_{i,shear}''' = \alpha_g \cdot F_{wl}''' \quad (7.3)$$

Ishii and Mishima [Ref. 9] also discussed this term and concluded that it should be expressed as follows:

$$F_{i,shear}''' = C \cdot \alpha_g \cdot F_{wl}'''$$

where the constant, C , was expected to have a value very close to unity. Therefore, in TRACE model, we evaluate the induced shear term using equation (7.3).

8. Model Verification and Assessment

The two-phase flow momentum equation has a few momentum sources other than the wall friction term (including interfacial friction among others). Consequently, TRACE predictions of the two-phase flow pressure drop and void fraction profile along a one-dimensional component depend on all momentum sources. We cannot simply assess a two-phase flow

experiment and then draw a conclusion regarding the accuracy of the wall friction model.

In this paper, we evaluated the wall drag model using a free-falling film flow down along a vertical pipe. For such a free-falling film flow, the available literature [Refs. 10–19] provides experimental data for dimensionless film thickness, which is defined as follows:

$$\delta^* = \frac{\delta_g^{1/3} (\rho_f - \rho_g)^{1/3} \rho_f}{\mu^{2/3}}$$

where δ is the dimensional film thickness and δ^* is the dimensionless film thickness.

We then develop a TRACE model to test the relationship of the dimensionless film thickness and the Reynolds number. Figure 5 depicts the nodalization of the model for annular film flow. In that figure, Break 2 supplies vapor, while Break 3 provides pressure boundary conditions at the exit end of Pipe 1. Pipe 1 has 20 volumes, each of which has a cell length of 0.1m. The pipe diameter is also set to 0.1m, which is much larger than the liquid film thickness in an annular film flow. The liquid velocity will reach a constant value along the wall after a certain distance. A side junction at Cell 2 is connected to a fill component, which has set liquid inlet velocities with step increases to simulate various film thicknesses with various Reynolds numbers. The film Reynolds number is then defined as follows:

$$Re = \frac{G_1 D}{\mu_l}$$

where G_1 is the liquid mass flux, D is the pipe diameter, and μ_l is the liquid viscosity.

The model computes the Reynolds number and dimensionless film thickness by using signal variables and control blocks for Cell 10 of Pipe 1. Figure 6 compares the TRACE predictions to the experimental data, showing that the TRACE predictions are reasonable; however, at low Reynolds numbers, the code underpredicts the film thickness.

Further investigation revealed that vapor moves faster than the liquid film because of the boundary setting. This relative velocity created an interfacial shear and caused the film thickness to be underestimated at low Reynolds numbers. The green line in Figure 6 shows that the TRACE code yields an excellent prediction

when the interfacial friction is turned off (by hard-wiring the code).

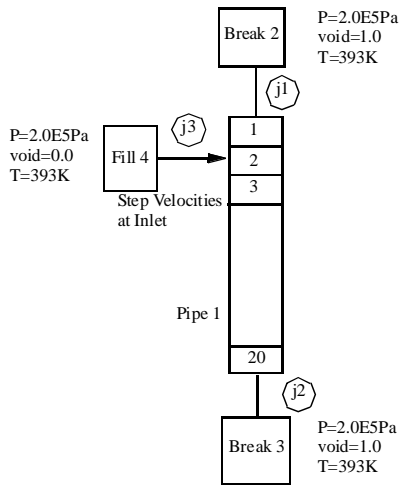


Figure 5: TRACE nodalization for annular film flow.

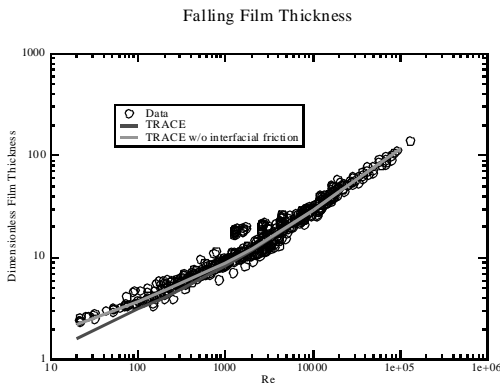


Figure 6: TRACE predicted film thickness compared to experimental data.

9. Summary and Conclusion

A new wall frictional drag package has been developed and implemented in the TRACE code to model the wall drag for two-phase flow system code. The modeled flow regimes are (1) annular/mist, (2) bubbly/slug, and (3) bubbly/slug with wall nucleation. The new models use void fraction (instead of flow quality) as the correlating variable to minimize the calculation oscillation. The annular/mist regime is subdivided into three separate regimes for pure annular flow, annular flow with entrainment, and film breakdown. In the bubbly/slug flow regime, a physically based model has been formulated for adiabatic conditions. Finally, for

bubbly/slug flow with wall nucleation, the bubbles are presented within the hydrodynamic boundary layer, and the two-phase wall friction drag is significantly higher with a pronounced mass flux effect. In addition, an empirical correlation has been studied and applied to account for nucleate boiling. Verification and validation tests have been performed for annular flow, and the test results showed a significant code improvement.

References

- [1] NUREG/CR-6722, "TRAC-M/FORTRAN (Version 3.0) User's Manual," U.S. Nuclear Regulatory Commission, Washington, DC, May 2001.
- [2] Churchill, S.W., "Friction-Factor Equation Spans All Fluid-Flow Regimes," *Chemical Engineering*, Vol. 84, No. 24, pp. 91-92, November 7, 1977.
- [3] Ferrell, J.K., and J.W. McGee, "A Study of Convection Boiling Inside Channels," Final Report, Volume III, North Carolina State University, Department of Chemical Engineering, Raleigh, NC, June 1966.
- [4] Yamazaki, Y and Shiba, M., "A Comparative Study on the Pressure Drop of Air-Water and Steam-Water Flows", Cocurrent Gas-Liquid Flow Proceedings of an International Symposium on Research in Cocurrent Gas-Liquid Flow Held at the University of Waterloo, Sept. 1968
- [5] Yamazaki, Y. and Yamaguchi, K., "Characteristics of Cocurrent Two-Phase Downflow in Tubes", *Journal of Nuclear Science and Technology*, Vol 16[4], pp 245-255, 1979.
- [6] Ferrell, J.K., and D. M Bylund, "A Study of Convection Boiling Inside Channels," Final Report, Volume III, North Carolina State University, Department of Chemical Engineering, Raleigh, NC, June 1966.
- [7] Collier, J.G. and Thome, J.R., "Convective Boiling and Condensation, 3rd Edition, 1996
- [8] Levy, S., "Forced Convection Subcooled Boiling Prediction of Vapor Volumetric Fraction", *Int. J. Heat Mass Transfer*, 10, pp 951-965, 1967.

- [9] Ishii, M and Mishima, K, "Two-Fluid Model and Hydrodynamic Constitutive Relations", Nuclear Engineering and Design, Vol 82, pp 107-126, 1984.
- [10] Belkin, H.H., A.A. MacLeod, C.C. Monrad, and R.E. Rothfus, "Turbulent Liquid Flow Down Vertical Walls," *AIChE Journal*, Vol. 5, pp. 245–248, 1959.
- [11] Collier, J.G., and G.F. Hewitt, "Film Thickness Measurements," AERE-R4684, United Kingdom Atomic Energy Authority (UKAEA), Harwell, England, July 1964.
- [12] Hawley, D.L., and G.B. Wallis, "Experimental Study of Liquid Film Fraction and Pressure Drop Characteristics in Vertical Countercurrent Annular Flow," EPRI NP-2280, Electric Power Research Institute, Palo Alto, CA, February 1982.
- [13] Hewitt, G.F., and G.B. Wallis, "Flooding and Associated Phenomena in Falling Film Flow in a Vertical Tube," AERE-R4022, UKAEA, Harwell, England, 1963.
- [14] Zabaras, G.J., and Dukler, A.E., "Countercurrent Gas-Liquid Annular Flow, Including the Flooding State," *AIChE Journal*, Vol. 34, No. 3, pp 389–396, 1988.
- [15] Gimbutis, G., "Heat Transfer of a Turbulent Vertically Falling Film," *Proceedings of the 5th International Heat Transfer Conference*, Vol. 2, pp 85–89, 1974.
- [16] Chien, S.F., "An Experimental Investigation of the Liquid Film Structure and Pressure Drop of Vertical, Downward, Annular, Two-Phase Flow," Thesis, University of Minnesota, 1961.
- [17] Chien, S.F., and W. Ibele, "Pressure Drop and Liquid Film Thickness of Two-Phase Annular and Annular-Mist Flows," *Journal of Heat Transfer*, pp 89–96, February 1964.
- [18] Webb, D.R., and G.F. Hewitt, "Downward Co-Current Annular Flow," *Int. J. Multiphase Flow*, Vol. 2, pp 35–49, 1975.
- [19] Tatsuhiro, U., and T. Toshihiko, "Studies of Liquid Film Flow in Two-Phase Annular and Annular-Mist Flow Regions," *Bulletin of the JSME*, Vol. 17, No. 107, May 1974.